Research Article

Sandhya Vidya Sagar Mudrakola[#], Chandra Lekha Koopari[#], Ramesh Kande, Karthik Rajkumar, Pawan Kumar Anoor, Sandeepta Burgula*, and Farhatullah Syed*

Synthesis and stabilization of anatase form of biomimetic TiO_2 nanoparticles for enhancing anti-tumor potential

https://doi.org/10.1515/gps-2023-0182
received September 15, 2023; accepted May 23, 2024

Abstract: The present study emphasizes the stabilization of the biologically active anatase form of titanium dioxide (TiO_2) nanoparticles (NP). TiO_2 NP require stringent conditions for chemical synthesis and are usually a mixture of biologically inactive bulk rutile and the active bulk anatase forms. We utilized the culture pellet of the *Exiguobacterium aestuarii SBG4 MH185868* to synthesize and stabilize the anatase form of TiO_2 NP. The NP showed λ_{max} at ~350 nm and scanning electron microscope micrographs indicated their oval and spherical shape. Steric stabilized anatase TiO_2 NP exhibited substantial cytotoxicity of up to 80% reduction in cell viability at 100 µg against cervical cancer derived HeLa and SiHa cell lines, whereas the rutile form showed least cytotoxicity. Clonogenic inhibition assay of HeLa cells showed dose-dependent decline with a 75% reduction in colony formation at 100 µg TiO_2 NP and cell migration assay revealed significant inhibition in recovery of the wound/scratch in presence of anatase form of TiO_2 NP (10–33% at 24 h and 42–79% at 48 h). Co-incubation of HeLa cells with anatase TiO_2 NP in chorioallantoic membrane of embryonated chick eggs prevented the formation of new capillaries (20 ± 5% compared with control groups), indicating appreciable anti-angiogenic activity of the NP. Further, TiO_2 NP tagged with doxorubicin and paclitaxel exhibited enhanced cytotoxicity against cancer cells at very low concentrations of 9 and 120 nM itself, indicating their anti-tumor potential. In conclusion, biomimetic anatase TiO_2 NP have significant anti-proliferative and anti-angiogenic activity and can have potential application in tagging with generic anti-cancer drugs for enhanced cytotoxicity against cancer cells.

Keywords: titanium dioxide, nanoparticles, clonogenicity, cell migration, anti-angiogenic activity

1 Introduction

Nanotechnology is one of the most intensely researched areas because of its wide range of potential applications in the fields of biomedicine, agriculture, environment, industries, cosmetics, food products, optics, and electronics. They are of great significance as they effectively act as a bridge between bulk materials and atoms or molecules [1].

Titanium dioxide (TiO_2) nanoparticles (NP), also known as ultrafine titanium dioxide, are believed to be one of the three most utilized nanomaterials, along with silicon dioxide and zinc oxide NP. They are used in diverse areas ranging from paints, plastics, sunscreens, cements, foods, cosmetics, surgical implants, drugs, and other products due to their impeccable UV absorption and photocatalytic sterilizing properties. The photocatalytic activity of TiO_2 NP can be used in decomposing organic compounds in wastewater [2,3]. In the field of nanomedicine, TiO_2 NP are currently under investigation for the treatment of acne, recurrent condyloma accuminata, atopic dermatitis, hyperpigmented skin lesions, and other nondermatological diseases [4].

Due to their exclusive chemical and physical properties, TiO_2 NP are manufactured on a large scale for industrial applications to meet the ever-increasing demand. Compared to NP produced by conventional means, which

# MVSS and CLK contributed equally to the manuscript.

* **Corresponding author: Sandeepta Burgula**, Department of Microbiology, Osmania University, Tarnaka, Hyderabad, 500007, India, e-mail: s_burgula@osmania.ac.in, tel: +91-40-27090661
* **Corresponding author: Farhatullah Syed**, Advance Cell and Gene Therapy Section, King Faisal Specialist Hospital & Research Centre (KFSH&RC), Riyadh, Saudi Arabia; Department of Microbiology, Osmania University, Tarnaka, Hyderabad, 500007, India, e-mail: fsyed@kfshrc.edu.sa
Sandhya Vidya Sagar Mudrakola, **Chandra Lekha Koopari**, **Ramesh Kande**, **Karthik Rajkumar**, **Pawan Kumar Anoor:** Department of Microbiology, Osmania University, Tarnaka, Hyderabad, 500007, India

are known for adverse effects on cell viability or physiology, biosynthesized NP have some exclusive properties and can be employed with minimum side effects when long term or chronic exposure is avoided [5]. In recent years, NP biosynthesis involving microorganisms or plant extracts, along with eco-friendly chemical procedures and mild conditions of temperature and pressure have been proposed. Bacteria can mediate the synthesis of NP because of their ability to reduce TiO_2 into NP form with minimum processing variables [6–10]. Keeping in view of the ubiquitous importance of titanium and environmental issues related to the production of TiO_2 nanopowders, the present work reports an eco-friendly approach for the synthesis of nano-Titania. The "biomimetic" method utilized in the study is supported by the fact that majority of the bacteria inhabit ambient environments of varying temperature, pH, and pressure; NP synthesized through these processes have higher catalytic reactivity, greater specific surface area and stability. Bacterial synthesis of TiO_2 NP can be both intracellular and extracellular. The intracellular method involves microbial enzymes, wherein NP are transported into microbial cells through metal ion transporters, whereas extracellular synthesis of NP involves trapping of the metal ions on to the cellular surface and their reduction in the presence of microbial enzymes [11]. A marine isolate *Exiguobacterium aestuarii SBG4 MH185868*, which was previously isolated and used for the synthesis of gold and selenium NP, has been utilized in this study [12]. Total cell lysate was used to synthesize the NP, which were characterized based on various structural properties, stability and storage conditions using common preservatives and evaluated for their biological activity.

Recent studies indicate that selenium, gold, silver, and magnetic NP may be used for targeted drug delivery in cancer therapy [13]. TiO_2 NP have versatile medical applications such as in joint replacement surgeries, topical emulsions, creams, oral medications, and surgical implant cancer therapy, due to their low toxicity [14]. Titanium exposure is generally considered harmless and least penetrative. However, its crystalline forms, namely, bulk anatase, rutile or bulk anatase–rutile forms, have varying biological activities. Rutile forms are known to be chemically inert and therefore have insignificant biological activity, whereas bulk anatase form is shown to be much more stable with appreciable bioactivity [4]. Several studies have indicated that the application of NP in medicine can synergistically improve the effectiveness of many existing therapies. Conjugation of drugs with NP can enhance their selective accumulation in diseased tissues. Since TiO_2 NP are non-toxic to normal cells and have high biological activity against cancer cells, they can be efficiently utilized by conjugation with cytotoxic drugs in cancer treatment. Preparation of TiO_2 NP by chemical synthesis is laborious, results in hazardous by-products, and requires high temperature and pressure. In addition, it results in a mixture of the inert rutile form and the bioactive anatase form. The main focus of the present study is biomimetic synthesis and optimization of TiO_2 NP in their bulk anatase form and their subsequent analysis of biological activity [15].

2 Materials and methods

2.1 Chemicals

All the chemicals and media components used in the study were purchased from Hi-Media (Mumbai, India) and Sigma-Aldrich (USA).

2.2 Cell lines

HeLa and SiHa cells were procured from National Centre for Cell Science, Pune, India, and propagated in Dulbecco's Modified Eagle's Medium (DMEM) high glucose (Gibco, USA), supplemented with 10% fetal bovine serum (FBS) and 1X, antimycotic (Himedia, India).

2.3 Experimental set up for titanium NP synthesis

Total cell protein (TCP) of *E. aestuarii SBG4 MH185868* was prepared from log 8 CFU ml^{-1} of cell pellet obtained from an overnight grown culture in tryptophan enriched banana peel extract (TEBP medium containing dried banana peel extract [8%, serving as both carbon and nitrogen source] enriched with tryptophan [0.2 mM], 10% – NaCl and pH – 6.5), which is a cost-effective culture medium developed at our laboratory and according to our previous protocol [12]. Brief procedure of TCP preparation involves the cultivation of *E. aestuarii* in TEBP at 37°C for 24 h. The culture supernatant was separated by centrifugation at 6,000×*g* for 10 min at 4°C and the total cell pellet obtained was utilized for NP synthesis.

The experimental set-up for parameter optimization was designed using 'one factor at a time' (OFAT) method to choose the dynamic variables, studying influence of one factor at a time, keeping the other factors constant and

their importance in synthesis of better quality TiO_2 NP. The parameters optimized were in the following sequence: first, TCP in varying concentrations (2.5–10%) was taken with rest of the parameters constant (200 mM salt, pH – 7.5, no preheating step), followed by the optimization of titanium dioxide salt in 25–200 mM range TCP – at pH – 7.5. Preheating of salt solution prior to the addition of TCP enhanced the synthesis [7]. The NP synthesized by optimized parameters were used for further characterization.

2.4 Characterization of NP

The TiO_2 NP synthesized after optimization were characterized by UV–Vis spectroscopy (Epoch, India) for their surface plasmon resonance (SPR) in the range of 300–500 nm [11] at a resolution of 1 nm to determine SPR absorbance maxima (λ_{max}). The NP samples with variable interactions were checked for the presence of functional groups using Fourier transform infrared (FTIR) analysis (SHIMADZU, India) at a resolution of 4 cm^{-1} in KBr pellets and analysis ranging in 400–4,000 cm^{-1}, to determine the vibration and rotation of molecules influenced by infrared radiation at a specific wavelength [16]. The *x*-axis of the spectrum represents the wave number while the *y*-axis represents absorbance or transmittance.

TiO_2 NP were centrifuged and applied onto clean glass slides and dried (process repeated multiple times until glass slide was completely covered with NP layer). The slides were used for X-ray Diffraction (XRD) analysis to confirm their crystalline nature (Philips X-pert pro, India) (40 kV and 30 mA current with 2.2 KW Cu anode radiation (k = 1.540 Å). The morphological analysis of the NP was carried out using scanning electron microscope (SEM) (Carl Zeiss, AG, India) with different magnifications. Energy dispersive X-ray spectroscopy (EDX) analysis of elemental TiO_2 NP was carried out with the same instrument from 0 to 12 keV [7]. The effective surface charges on the TiO_2 NP at different variables like pH and steric stabilized NP potentials and polydisperse index values were measured using zeta analyser (Horiba scientific, NP analyser SZ-100) [17].

2.5 Formulation for steric stabilization

The TiO_2 NP were synthesized as described earlier, followed by nanosuspension preparation in sterile distilled water subsequently stabilized by adding 1% (w/v or v/v) of polymers like polyethylene glycol (PEG-4000) and glycerol, ethyl alcohol, Tween-20 (non-ionic surfactant), and hydrochloric acid – 0.1 N (HCl as buffering agent). These compounds act as stabilizers, emulsifiers, tonicity adjusters, and cryo-protectants for long-term storage and preventing agglomeration due to steric stabilization [18,19]. PEG, glycerol, or Tween 1% (w/v or v/v) were either used individually or in combination with HCl or ethyl alcohol or both with above-mentioned stabilizers are represented in Table 2. After adding stabilizers to the NP, suspensions were homogenized and kept in an orbital shaker at 120 rpm, at room temperature for 5 h, to ensure the homogeneity followed by preservation at 4°C [11]. The stability was checked every 5 days of preservation, and after 3 months, the samples showing good stability in terms of SPR absorption maxima (λ_{max}) were analyzed for Zeta potential.

2.6 Biocompatibility – *in vitro* analysis of NP

2.6.1 Cytotoxicity

The cytotoxicity of TiO_2 NP in both rutile (pH – 7.5) and anatase (pH – 9.0) forms was assessed in the cervical cancer cell lines, HeLa and SiHa, and human foreskin fibroblast (HFF) cell line (normal cell line) by performing the 3-(4,5-dimethylthiazol-2-yl)-2,5-diphenyltetrazolium bromide (MTT) assay [20]. Approximately 15,000 cells per well (HeLa) were seeded in a flat-bottomed 96-well plate supplemented with 200 µl of Dulbecco's Modified Eagle Medium (DMEM) + 10% Fetal Bovine Serum (FBS) and incubated in a 5% CO_2 incubator at 37°C for 24 h. The spent media was replaced with fresh serum-free media and incubated for 8 h. The cells were then treated with increasing concentrations of both TiO_2 NP forms (1–100 $\mu g \cdot ml^{-1}$). Each set of concentrations was maintained in triplicates and after 24 h of incubation, the cells were replaced with fresh DMEM containing MTT (0.5 $mg \cdot ml^{-1}$) for reduction by metabolically active cells, in part by the action of dehydrogenase enzymes, to generate reducing equivalents such as NADH and NADPH. The plate was incubated for 4 h in the dark, after which medium was removed and 100 µl of dimethyl sulfoxide (DMSO) was added to each well. The plate was kept in dark for 5 min and the optical density (OD) was measured at 570 nm using microplate reader (Agilent, USA) (to calculate cytotoxicity using the following equation:

$$\text{Cytotoxicity}(\%) = \frac{(\text{control OD} - \text{sample OD})}{\text{control OD}} \times 100 \quad (1)$$

2.6.2 Clonogenic inhibition assay

Clonogenic assay or colony formation assay is an *in vitro* cell survival assay based on the ability of a single cell to grow into a colony. HeLa cells seeded onto a six-well plate

(1×10^4 per well) were treated with TiO_2 NP (5–100 μg·ml^{-1}), according to the protocol described by Rafehi et al. with slight modifications [20,21]. The treated cells were incubated in 5% CO_2 at 37°C for an incubation period of 7–10 days and observed for visible colony formation. After appropriate incubation time, cells were fixed and stained. A brief procedure for fixing and staining involves removing the spent media and washing with Dulbecco's phosphate-buffered saline (DPBS) followed by fixing with 5 ml of 10% neutral buffered formalin solution for 15–30 min. Five milliliters of 0.01% (w/v) crystal violet was immersed in distilled water for 30–60 min. Excess crystal violet was washed with DPBS, and the plate was left for drying. Cell counting was performed using ImageJ software (Fiji Version 1.5a), and the percentage of clonogenic inhibition was calculated.

2.6.3 Cell migration assay

HeLa cells were cultivated in a six-well plate until they reached a single-layer confluency and the linear wounds or scratches were made gently using 10 μl micropipette tips [22]. The cells were washed with Dulbecco's phosphate-buffered saline (DPBS) and incubated in fresh media at 37°C for 48 h. The wound was monitored by a microscope (EVOS Cell Imaging systems, Thermo Scientifics, India) and gap widths were measured using ImageJ (Fiji version 1.5a) software. Scratch width percentage was calculated to determine the cell migration at different concentrations of TiO_2 NP.

2.6.4 Hen egg chorioallantoic membrane (CAM) assay

The anti-angiogenic property of biomimetic TiO_2 NP was investigated using embryonated hen egg CAM layer as an *in vivo* model. Briefly, fertilized chicken eggs were procured (Venkateshwara Hatcheries Pvt Ltd, Telangana, India) and incubated at 37°C under 80% humidity from days 7 to 11. On day 11, the eggs were surface sterilized using surgical spirit, and the blood vessels were marked using an egg candler. A minute hole was made using a sterile needle along the side of the egg. One million (1×10^6) HeLa cells in approximately 100 μl of DPBS were injected carefully on to the CAM layer using an insulin syringe and sealed with latex wax [23], After 72 h of incubation, the cells were harvested by gently breaking the egg shell and carefully separating the CAM layer placed onto a Petri dish. Changes in angiogenesis were quantified by counting the number of new blood vessels branching out of the main vessel. The anti-angiogenic effect of NP is calculated as the relative number of arterial branches compared with appropriate controls.

2.6.5 Synthesis of nanoconjugates and cytotoxicity analysis on HeLa cells

Concentrations ranging from 0.05 to 1.8 μM of doxorubicin (DX) and 0.03–1.2 μM of paclitaxel (PTx) were added to TiO_2 NP (1.25 μM) and incubated at room temperature for 24 h. After 24 h of incubation, the reaction mixture was centrifuged at 8,000 rpm, unbound or excessive drug was aspirated, and pellet was resuspended in PBS. The tagging of drugs was confirmed by SPR band by the absorbance and comparison of tagged NP to bare TiO_2 NP [24]. The cytotoxicity of the DX-loaded NP, PTx loaded NP, and bare NP was evaluated by the MTT assay [20].

2.6.6 Statistical analysis

All the optimizations and *in vitro* and *in vivo* studies were performed thrice independently and in triplicates for each treatment. The resultant data were evaluated by ANOVA –single factor ($p < 0.05$).

3 Results and discussion

The present study utilizes the marine bacterial isolate *E. aestuarii SBG4 MH185868*, previously isolated at our laboratory to synthesize titanium dioxide NP by employing the TCP of *E. aestuarii SBG4* [11].

3.1 Optimization of process parameters

The reduction of metallic salts into the corresponding NP depends on several factors. The first crucial step involves reducing components of TCP that induce biomineralization, the concentration of the precursor metallic salt, and environmental conditions such as pH and temperature. All these conditions influence NP size, morphology, and functional groups stabilizing the TiO_2 NP. Hence, it is crucial to optimize these factors individually during biosynthesis to increase the overall quality and efficiency of particles [25]. The synthesis of nanosized TiO_2 colloidal particles was thus confirmed with SPR absorbance maxima (λ_{max}) ~350 (Figure 1a–d),

3.2 TCP size

The quantity of biological derivatives involved in the capping of NP synthesis and stabilization of TiO_2 NP requires optimization [26]. The *E. aestuarii SBG4* cell pellet obtained

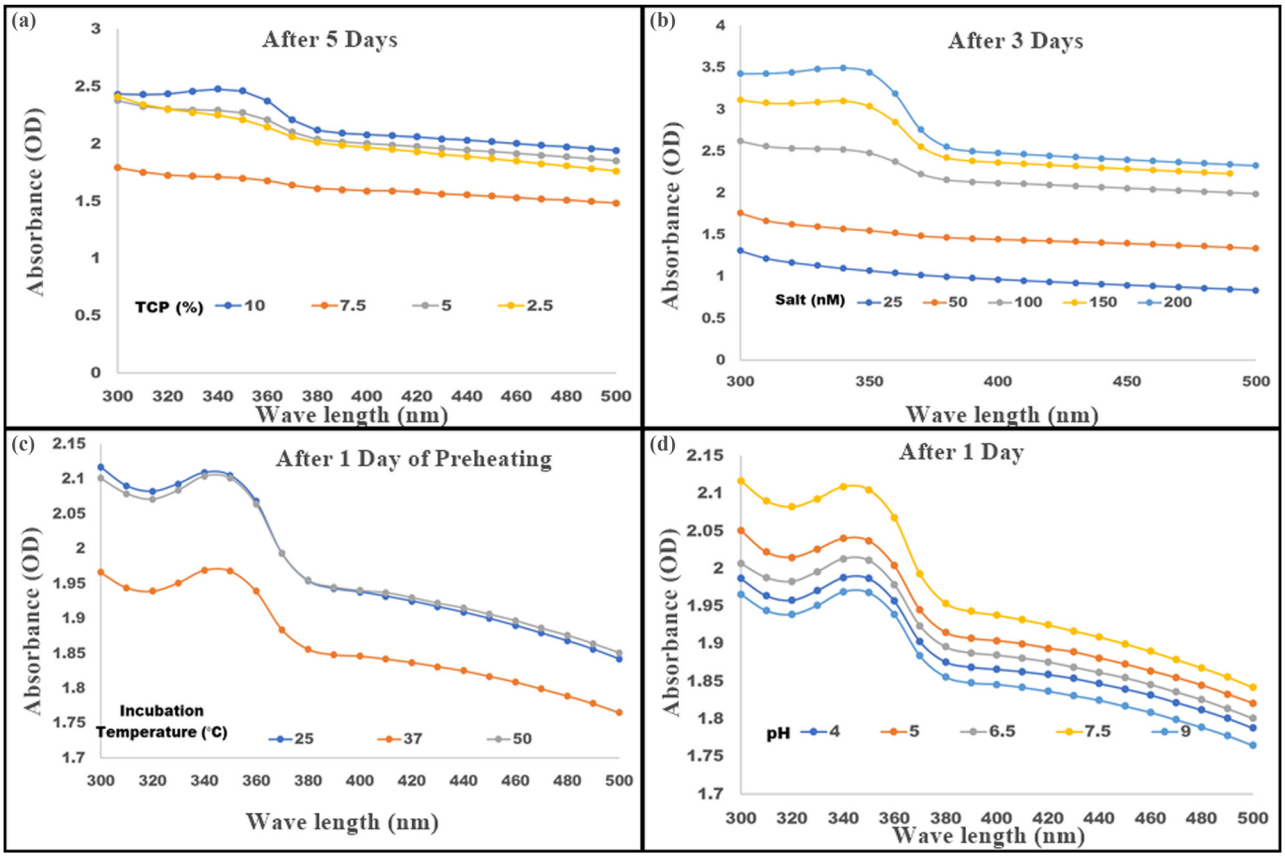

Figure 1: Biogenic TiO_2 nanoparticles were synthesized by incubating TiO_2 (100 mM) with total cell protein (TCP) obtained from *E. aestuarii* SBG4 MH185868 culture. The quality of the nanoparticles was assessed by measuring their λ_{max} while changing various parameters as shown at the end of synthesis. (a) Optimization of TCP percentage using 100 mM of TiO_2 salt on day 5 of incubation. (b) Optimization of TiO_2 salt concentration −25–200 (mM) with fixed TCP concentration on day 3. (c) Effect of preheating followed by incubation at varying temperatures for the synthesis of TiO_2 NP at optimized TCP and TiO_2 concentration. (d) Effect of varying pH on TiO_2 NP production after optimized preheating conditions with optimized TCP and TiO_2 concentrations.

after 24 h culture grown in TBPE was used for the synthesis of TiO_2 NP. The TCP of the cell pellet was used in a range of 2.5, 5.0, 7.5, and 10% (volume of culture used to obtain TCP). Among these, 10% TCP demonstrated optimum NP synthesis with 100 mM of TiO_2 salt concentration, when incubated for 5 days and the milky white colloidal solution indicated synthesis of TiO_2 NP, which were analyzed by measuring SPR absorbance maxima (λ_{max}) ~350 represented in Figure 1a [20]. Further optimization of TiO_2 NP synthesis was carried out with the aim to obtain nanospheres with appreciable biocompatibility, uniform size and shape, and so on. In addition, shortening the duration of synthesis was the focus of next experiments to prevent undesirable changes in NP due to prolonged incubation, such as aggregation/agglomeration and denaturation of TCP components responsible for the reduction of TiO_2 [18,19].

3.3 Optimization of salt precursor concentration

The titanium dioxide salt (precursor salt) concentration has significant effect on the biosynthesis of NP. To analyze the effect of TiO_2 salt concentration for NP synthesis, varying concentrations of TiO_2 salt were used, ranging from 25 to 200 mM and incubated at time intervals of 24 h from days 1 to 5 at 37°C (Figure 1b). Optimum λ_{max} was observed for synthesized NP at day 3 at 200 mM TiO_2 concentration, which did not change subsequently by day 5. This indicates the optimization and shortening of duration of NP synthesis from 5 days to 3 days at 200 mM of TiO_2 concentration. The results signify that the precursor salt has a vital role in optimal yield of NP and shortening the duration of synthesis [25].

3.4 Effect of preheating and temperature for the synthesis of NP

After optimization of salt concentration, further studies were conducted to decrease the duration of synthesis of TiO_2 NP. Titanium dioxide is amorphous and thermostable in nature and must be properly solubilized for a uniform distribution during NP synthesis using TCP. Solubilization of TiO_2 was aided by preheating at 50°C for 30 min, followed by the addition of 10% TCP after which the mixture was incubated at various temperatures (25, 37, and 50°C). The synthesis of NP was confirmed by recording λ_{max} change in Figure 1c. Preheating contributed to the shortening of duration from 3 days to 1 day after optimization of salt concentration. After preheating, incubation at various temperatures did not show much effect on NP synthesis, which can be observed in terms of the absorption maxima and uniformity of the observed peaks at all temperature (25, 37, and 50°C). Further synthesis of TiO_2 NP was carried out at 37°C after preheating.

3.5 Effect of pH on the biogenic synthesis of TiO_2 NP

The pH and redox potential of membrane proteins play a vital role in activation of membrane bound oxidoreductases, which provides a favorable condition for reduction of TiO_2 salt concertation to TiO_2 NP [7]. In the current work, we have focused on influence of pH on controlled NP synthesis. Prior to the addition of 10% TCP, sterile distilled water adjusted to various pH values ranging from 4.0 to 9.0 was utilized, followed by the addition of 200 mM TiO_2 salt and 10% TCP and incubated at 37°C for 24 h (1 day). Figure 1d represents the NP synthesis at varying pH values. pH 4.0, 7.5, and 9.0 were further characterized by XRD, SEM, and zeta potential, and pH 5.5 and 6.5 were omitted due to presence of aggregation of NP.

3.6 Characterization of TiO_2 NP

3.6.1 Nature and morphology of TiO_2 NP

To understand the influence of pH on crystalline nature of the TiO_2 NP, XRD analysis for the NP were synthesized by the following optimized conditions: preheating TiO_2 salt (200 mM) solution at 50°C at pH 4.0, 7.5, and 9.0 using 10% TCP was utilized. XRD analysis exhibited 2θ (°) and lattice plane of 25.22 (101) plane was identified as standard peak representing the only rutile form at a size of 14.77 nm at pH – 4.0 (Figure 2a), whereas Figure 2b represents pH – 7.5 with 2θ (°) and lattice plane 25.58 (101), 29.48 (100), 42.33 (111), 44.19 (210), and 62.89 (204), confirmed mixture of bulk rutile nature, and size range of 12–100 nm. At pH 9.0, bulk anatase was the predominant form with characteristic peak at 25.3 (101) followed by 37.8 (004), 48.07 (200), 53.8 (105), 55.08 (211), 62.7 (204), and 75.02 (215), which are the planes in a size range of 18–27 nm (Figure 2c) [26]. The pattern obtained in the study fits well with the data of Joint Committee for Powder Diffraction Studies (JCPDS). The XRD spectra for TiO_2 NP revealed the 2θ (°) values (Figure 2d) and the spectra demonstrated broad diffraction peaks indicating very small sized crystallite. Though the rutile form is a more stable crystallite compared to anatase, anatase is known for its metastability, which means that it can transform to rutile at certain temperature and additionally has biological activity.

The morphology of rutile and anatase NP revealed by SEM analysis and micrographs confirms the spherical shape of TiO_2 NP produced by *E. aestuarii SBG4 MH185868* at different pH values 4.0, 7.5, and 9.0 (Figure 3a–c). An average size of TiO_2 NP reported at various pH are 4.0–70: ±10 nm and 7.5 and 9.0: 60 ± 5 nm (Table 1). Homogeneity of the nanospheres was observed with the grain size falling mostly in submicron range and the EDX revealed the presence of elemental titanium (Figure 3d) [7].

3.6.2 Stability of TiO_2 nanosuspension

Zeta potential is an indicator of physical stability of nanosuspensions which is a result of the degree of repulsion between similarly charged particles in the formulation that prevents particle aggregation during storage [27]. In this study, zeta potential of NP synthesized at various pH conditions and steric stabilized nanosuspensions of both anatase and rutile forms were analyzed and polydisperse index (PDI) values and surface charge of particles were determined to check if nanosuspensions were monodisperse or polydisperse.

3.6.3 Influence of pH on zeta potential during synthesis

The zeta potential of NP synthesized at various pH conditions were found to have maximum potential >−70 mV and PDI in the range of 0.5–0.7, due to strong repulsive forces [28]. The zeta potentials were measured as – pH 4.0: −78 mV, pH 7.5: −73 mV, and pH 9.0: −76 mV (Table 1).

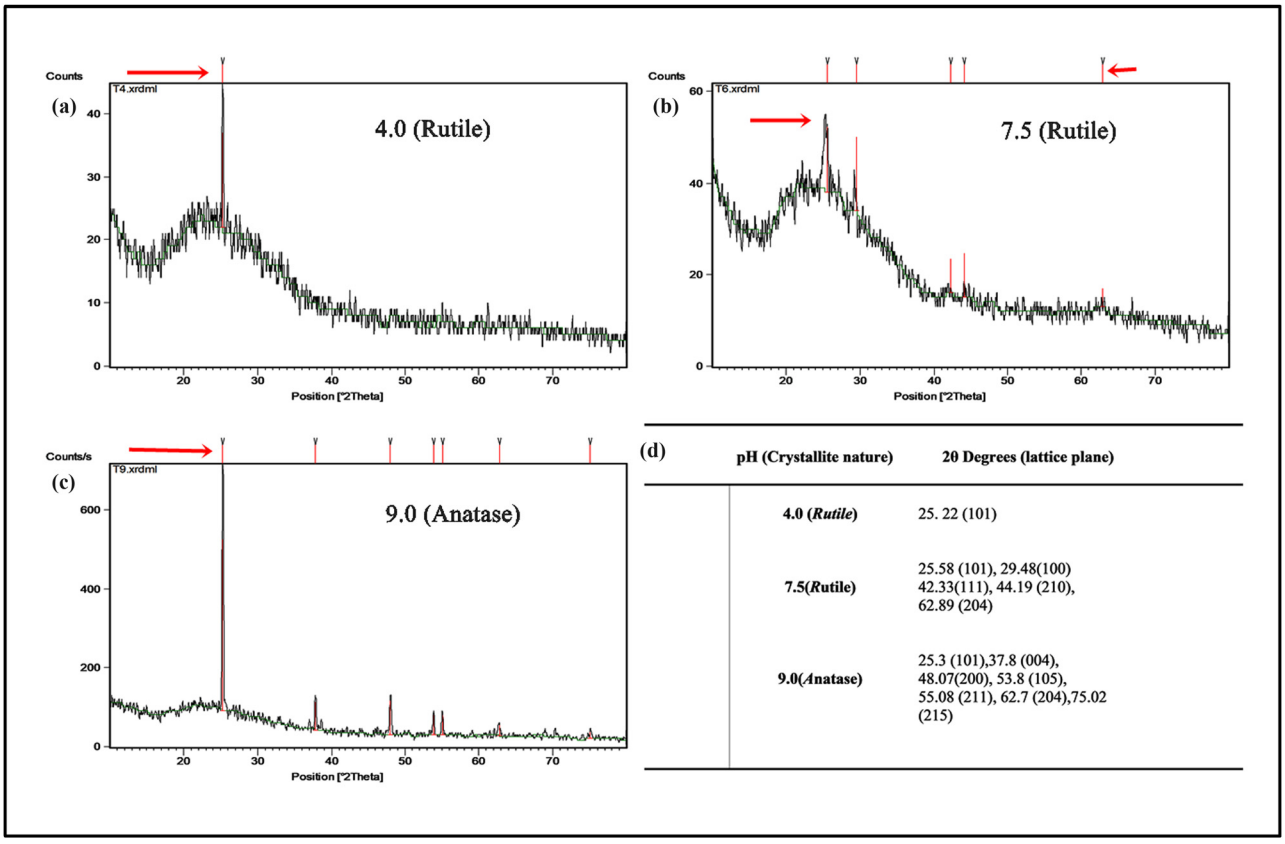

Figure 2: X-ray diffraction analysis of TiO_2 NP synthesized using *E. aestuarii SBG4MH185868* showing 2*θ* values. The spectra demonstrated broad diffraction peaks indicating very small sized crystalline nature of TiO_2 NP synthesized at (a) pH 4.5 (rutile phase), (b) pH 7.5 (major rutile form), and (c) pH 9.0 (Major anatase form). (d) A list of 2*θ* values obtained at pH 4.5, 7.5, and 9.0.

Among all the values, pH 7.5 showing bulk rutile form and pH 9.0 showing bulk anatase form had acceptable PDI values of ~0.5, which represents monodisperse nature of the nanosuspension, whereas pH 4.0 showed PDI values >0.5 indicating their polydisperse nature. Hence, bulk rutile (pH – 7.5) and bulk anatase (pH – 9.0) forms were selected for further studies. During long-term refrigeration of NP, the phenomenon of Brownian movement in colloidal suspensions leads to the aggregation of NP in aqueous suspension. A similar observation was made when dried NP were resuspended in water [29]. In this context, nanosuspensions with various known cryoprotectants were tested for steric stabilization of NP as explained below.

3.6.4 Influence of steric stabilizers during preservation

The zeta potential of steric stabilized nanosuspensions are usually reported to be low, around −28 to −2 mV or even nearer to zero. Low zeta potential does not impact NP aggregation [19,23]. The stabilizer forms a layer around the NP which may decrease the attraction between the particles leading to decline in zeta potential, but it tends to increase the steric distance between the particles there by increasing the hydrophilicity and prevention of particle aggregation during long term storage conditions [29,30]. In the current study, the compounds used for steric stabilization were PEG, glycerol, and Tween-20 1% (w/v or v/v) which were tested individually along with HCl or ethyl alcohol for testing synergetic effect (Table 2). As a primary step for analysis, all the sets of formulations were observed for aggregation, followed by measuring SPR absorption maxima (λ_{max}) using spectral scanning. A shift in absorbance peak in SPR band either red or blue (rutile/anatase) represents a decrease/increase in the refractive index surrounding the NP due to the modification by different stabilizers [31–33]. The formulations showing constant λ_{max} ~350 nm were considered to have good stability and were further analyzed for zeta potential. The colloidal solution treated with HCl lead to precipitation and it was not considered as stabilizing due to a shift in the SPR λ_{max}. The combined effects of stabilized nanosuspensions

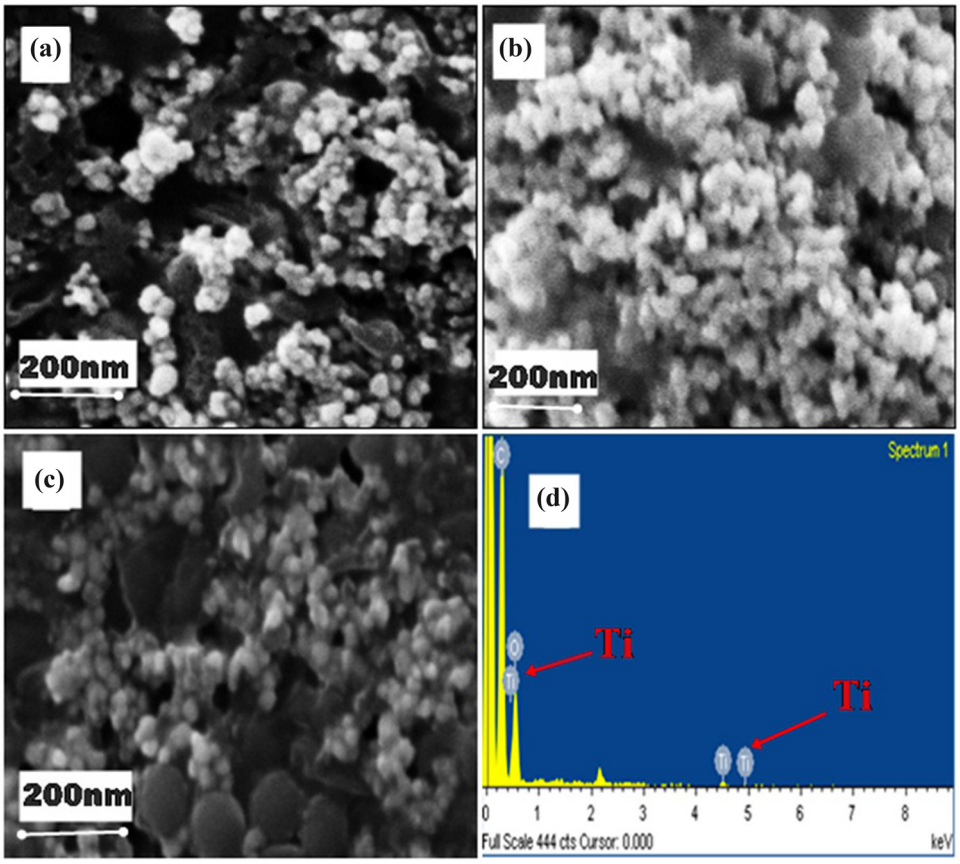

Figure 3: Scanning electron micrographs (SEM) of TiO_2 NPNp synthesized using *E. aestuarii SBG4 MH185868* at 200 nm resolution, showing spherical morphology of NP synthesizsed at different pH (a) pH − 4.0, (b) pH − 7.5, and (c) pH − 9.0, respectively. (d) EDX data confirmed the presence of Titanium.

Table 1: Influence of pH on stability of biogenic TiO_2 NP synthesis as observed by X-ray diffraction and measurement of zeta potential

Influence of pH					
S. no	**pH**	**Crystallite nature (XRD)**	**Zeta potential (mV)**	**PDI**	**Average particle size (nm)**
1	4.0	Rutile	−78.1	0.6	88 ± 10
2	6.5	Rutile	−71.0	0.6	90 ± 10
3	7.5	Bulk Rutile	−73.0	0.5	51 ± 10
4	9.0	Bulk Anatase	−76.0	0.5	61 ± 10

Table 2: Influence of steric stabilizers on biogenic TiO_2 NP synthesis assessed by measurement of zeta potential

Influence of steric stabilization						
S. no	**Bulk crystallite nature**	**Steric stabilizer**		**Zeta potential (mV)**	**PDI**	**SPR (λ_{max} – nm)**
1	Rutile	PEG	+ Ethyl	−24.70	0.1	360
2	Anatase		alcohol	−17.30	0.07	360
3	Rutile	Glycerol		−25.47	0.1	350
4	Anatase			−22.45	0.1	350
5	Rutile	Tween		−64.20	0.3	350
6	Anatase			−15.10	0.08	360

outperformed those of individual stabilizers. Specifically, nanosuspensions stabilized with PEG and ethyl alcohol exhibited zeta potentials of −24.7 mV for the rutile form and −17.3 mV for the anatase form, consistent with findings from earlier research [33]. Additionally, the SPR λ_{max} shifted by 5–10 nm from 350 nm, with a PDI of 0.1 for rutile and 0.07 for anatase. Given that glycerol, like PEG, is an effective and cost-efficient dispersing agent, we also used it in combination with ethyl alcohol. This resulted in shift in zeta potential to −25.47 mV for rutile and −22.45 mV for anatase. SPR absorbance shift was not observed for both the forms and PDI values were ~0.1, which represent monodispersing environment in the formulation even after long term storage for 2 months [30]. As glycerol tends to increase positive charge on the particles therefore the potential charge increases from > −73 ± 3 to −21 ± 2 mV and since glycerol is a smaller molecule than PEG, it did not alter the SPR λ_{max}, which confirms that

morphology is unaltered. Tween-20 which is a non-ionic surfactant [12] did not show promising results with anatase form of TiO_2 NP (−15.1 mV, PDI value 0.08) individually or in combination with ethyl alcohol, even though rutile form showed excellent stability (−64.2 mV, PDI value 0.3) with Tween-20 + ethyl alcohol [19]. Rutile form was stable in the presence of all the three stabilizers, but the anatase form was best stabilized by glycerol in combination with ethyl alcohol which was concluded using zeta potential values and observed values for PDI, SPR λ_{max}, and visual difference in particle aggregation. Based on these observations, the combination of glycerol with ethyl alcohol was concluded as the best cryoprotectant stabilizer for prolonged storage of TiO_2 NP.

3.6.5 FTIR analysis

The spectral FTIR analysis of biogenically synthesized TiO_2NP (Figure 4a and b) reveals the functional groups (carboxyl, hydroxyl, amines, and amide) which stabilize the NP by capping around the nanospheres. The IR spectrum shows the functional groups by characteristic intense peaks of at 3,524.06, 3,443.05, and 3,421.83 cm^{-1} for rutile form and 3,419.9 and 3,441.12 for anatase form corresponding to the surface water molecules and interacting hydroxyl group (Ti-OH) [14]. The 2,453.54 cm^{-1} of rutile and the 2,474.75 and 1,842.08 cm^{-1} of anatase peak correspond to C–H stretch. The rutile peaks around 1,629.90, 1,545.03, 1,500.67, 1,469.81, 1,442.8, 1,431.23 to 1,028.09 cm^{-1} signals and anatase peaks around 1,629.90, 1,491.02, 1,469.81, 1,383.01 to 1,051.24 cm^{-1} stretch represent C═O and strong stretching of N–H vibrations due to the presence of amide and amine groups around the nanospheres. Signals close to 1,261.49 cm^{-1} correspond to the C–O stretch vibrations, possibly due to the presence of an alcohol or carboxylic acid group. The C–N stretching vibrations of aliphatic amine signals were obtained around 1,051.24 cm^{-1}. The signals in the range of 669.32–472.58 cm^{-1} represent vibrations for TiO_2 NP due to the Ti–O–Ti bond, and intense peak around 669.32 cm^{-1} denotes rutile form and 561.30 cm^{-1} as anatase form, which agrees with the XRD spectra. The above information therefore indicates the contribution of components of total cell lysate in stabilizing and capping of the NP [8].

3.6.6 Biocompatibility and *in vitro* toxicity of rutile and anatase forms

After characterization of the crystalline rutile and anatase forms of TiO_2 NP, they were assessed for biological activity in terms of toxicity by MTT assay, wound healing assay, clonogenic cell proliferation assay, etc. Previous studies headed by Chahardoli et al. demonstrated significant antitumor activity in breast cancer and melanoma cells when TiO_2 NP were tagged with plant extracts or biomolecules like quercetin, caffeic acid, trans-ferulic acid, etc., in both rutile and anatase forms [33–36]. Several studies have indicated the crystal structure of TiO_2 NP in anatase forms to have higher cytotoxic activity due to its hexagonal crystal structure coordinated with oxygen [37]. This results in its high photocatalytic activity and ability to generate high amounts of reactive oxygen species (ROS) and enhanced cytotoxicity. To understand the ability of the anatase TiO_2 NP, further experimentation was therefore carried out.

3.7 Analysis of cytotoxicity of TiO_2 NP

As reported by several studies, NP such as gold, silver, selenium, titanium, and platinum exhibit anti-proliferative activity in cancer cells and tend to inhibit cancer progression [38]. Since TiO_2 NP demonstrated good shape and stability, we further analyzed their cytotoxicity against HeLa and SiHa (cervical cancer) cell lines. The decrease in cell viability or an increase in cytotoxicity may be due to apoptosis induced by the NP [39]. HeLa and SiHa cells exposed to TiO_2 NP (1–100 $\mu g \cdot ml^{-1}$) showed dose-dependent cytotoxicity (Figure 5) in anatase form, where cytotoxicity was observed at even low concentrations of 5 $\mu g \cdot ml^{-1}$ and to a degree of up to 80% at a higher concentrations of 100 $\mu g \cdot ml^{-1}$. Rutile form in general is inert and therefore showed minimum cytotoxicity, whereas anatase form seems to show significant cytotoxicity, probably by inducing the release of high amounts of ROS due to intracellular damage [38,40] Interestingly, HFF cells, which are non-cancerous normal cell line model, were unaffected by the NP indicating that they may have selective toxicity against cancer cells. The IC_{50} value for the anatase form was observed to be 6 $\mu g \cdot ml^{-1}$. Hence, the stabilized anatase form has high cytotoxicity even at low concentrations and has a good potential for anti-cancer application. Since the NP showed similar effects of toxicity against both HeLa and SiHa cells, further studies were conducted on HeLa cells. Mainly, analyses were performed to confirm the biological activity of the bulk anatase form.

3.8 Clonogenic assay

The colony formation assay or clonogenic inhibition assay is the method to determine cell reproductive death or cell

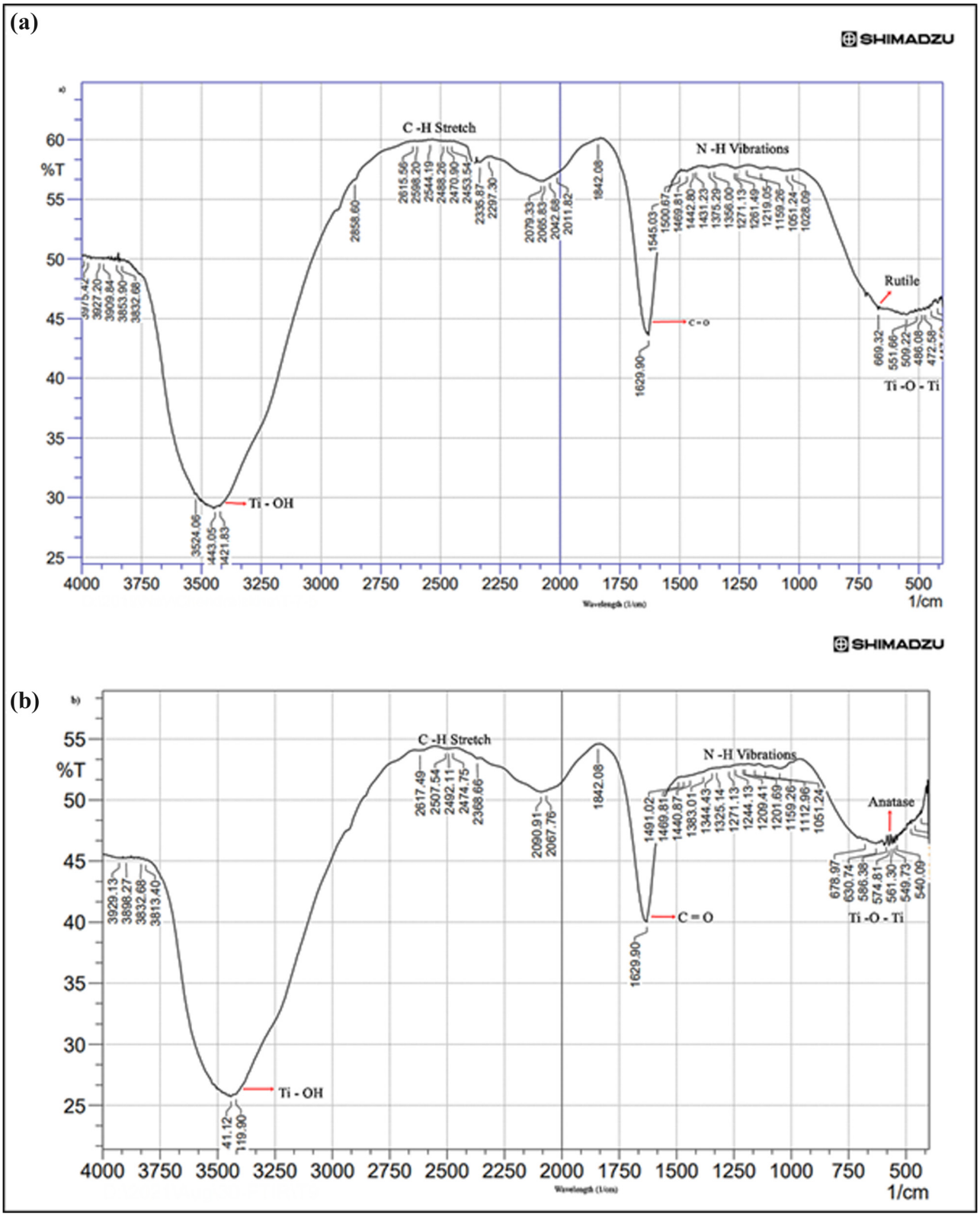

Figure 4: FTIR spectra of TiO_2 NP after optimization of pH, preheating temperature and TCP concentration. The analysis revealed the functional groups involved in the nanosphere formation and the presence of reducing groups responsible for the reduction of TiO_2 NP. (a) Rutile form and (b) anatase form.

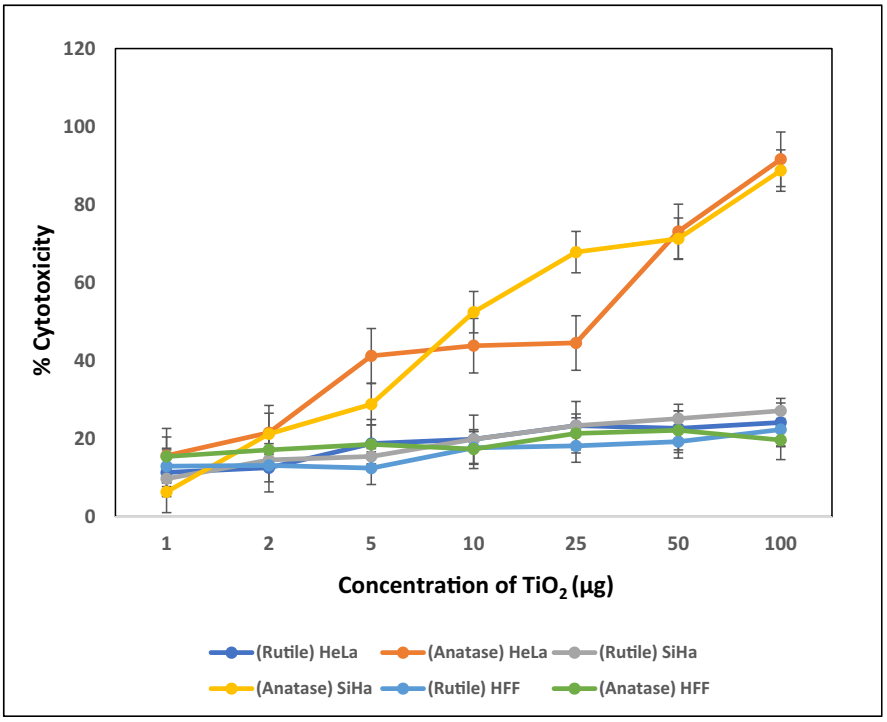

Figure 5: Graph depicting the effect of biogenic rutile and anatase TiO_2 NP on cervical cancer cell lines – HeLa and SiHa, as assessed by the MTT assay.

proliferation in the presence of any agent, such as in this study, TiO_2 NP. The assay performed using anatase form of TiO_2 NP showed exponential effect on the relative colony formation capacity of growing HeLa cells in a dose-dependent manner. Anatase TiO_2 NP treatment enhanced cell death and inhibited colony formation capability on HeLa cell population (Figure 6a). The decline in relative colony formation was found at concentrations starting from 50 $\mu g \cdot ml^{-1}$ at 50% and decreased to 25% at 100 $\mu g \cdot ml^{-1}$ (Figure 6b). Several previous studies have reported clonogenic inhibition in the presence of NP, although at higher concentrations, ranged above 100 $\mu g \cdot ml^{-1}$. Furthermore, most studies have utilized surface-modified NP comprising known anti-cancer molecules, such as DX. Here, we report the use of bare bulk anatase form of TiO_2 NP showing significant clonogenic inhibitions, especially at lower concentrations with minimal cytotoxicity to normal cells [41].

3.9 Suppressed HeLa cell migration

Cell migration and invasion play an important role in disease progression in cancer, which translates to metastatic effect of malignancy. Many forms of cancer, although treatable, fail to prevent remission in patients undergoing chemotherapy and recovering temporarily. This is due to invasive and metastatic activity of malignant cells, which remain dormant, hiding in visceral organs and resulting in metastasis over a period. With incidence of cancer rising every year all over the world, there is an urgent requirement of alternatives to suppress metastatic properties of cancer cells [42]. In this context, bulk anatase TiO_2 NP were used to test the effect on migration and invasiveness of HeLa cells. The NP showed significant inhibition on invasiveness of HeLa cells as observed from the prevention of recovery of wound/scratch [40]. The ability of HeLa cells to proliferate for covering the wound decreased drastically in the presence of anatase form of TiO_2 NP (10–33% at 24 h and 42–79% at 48 h) when compared with untreated cells, which showed up to 60% recovery of wound at 24 h and 90% at 48 h (Figure 7a and b) [37]. It is possible that the NP have cytotoxic effects that cause increased ROS generation, resulting in reproductive efficiency of cancer cells, thereby resulting in inhibition of cell migration [40].

3.10 *In vivo* model system for anti-angiogenic effect of TiO_2 NP

Since it was observed that the anatase TiO_2 NP in bare form could exert cytotoxicity, exhibit clonogenic inhibition, and inhibit cell migration, further investigations to understand if the anatase form can prevent angiogenesis were analyzed. For this, *in vivo* model of fertilized hen egg was

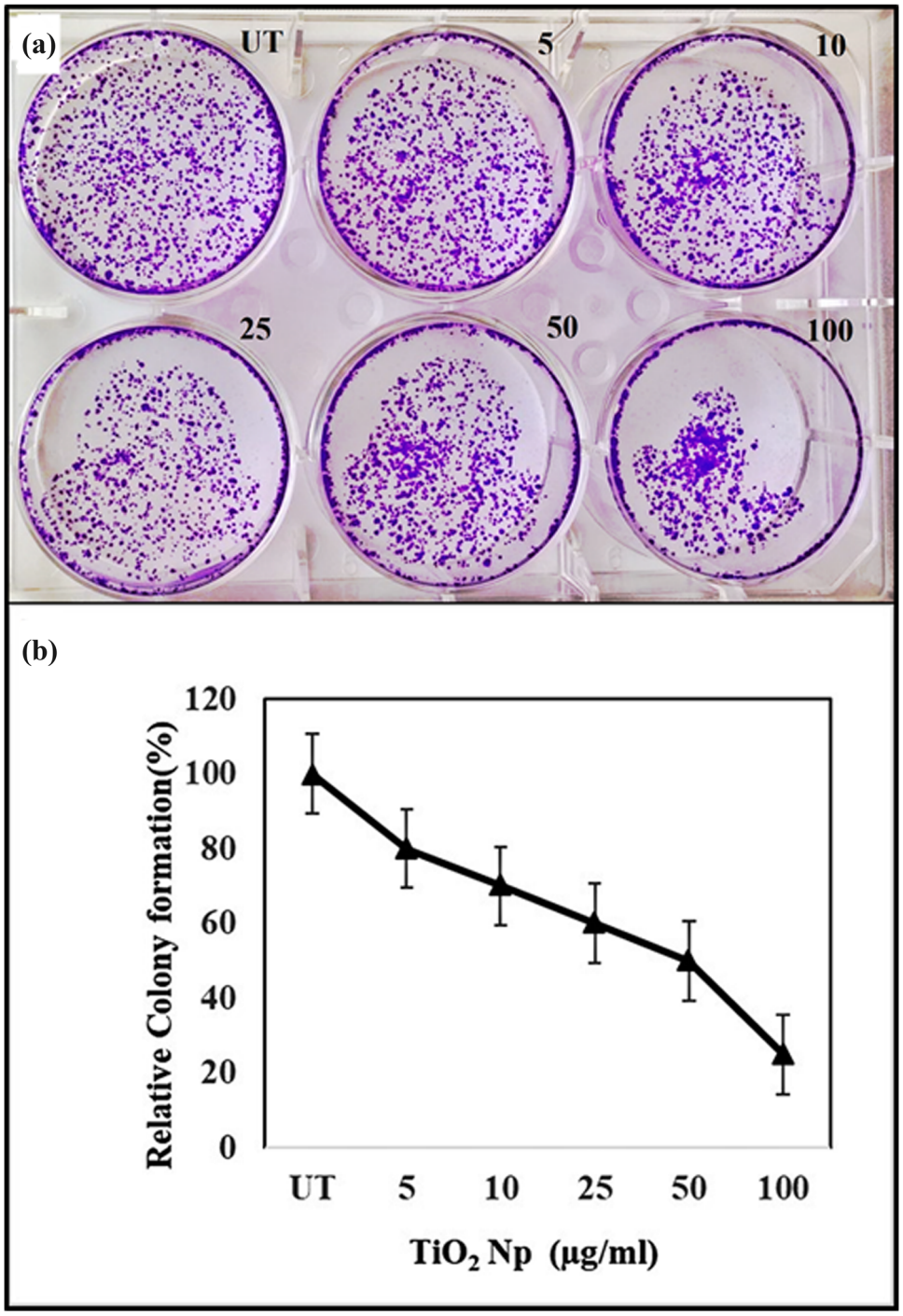

Figure 6: Dose-dependent inhibition of HeLa cell proliferation upon treatment with biogenic TiO_2 NP, as assessed by clonogenic assay. (a) Representative images of HeLa cell colonies obtained post 7 days treatment with TiO_2 NP and analyzed for effect on single-cell clonal proliferation after colonies were stained with crystal violet. (b) Quantification of the results.

used to carry out CAM assay. The CAM of 11-day-old eggs was overlaid with HeLa cells in the presence of TiO_2 NP and formation of new capillaries around the HeLa cells grafted around the CAM layer was analyzed (Figure 8a and b). Since HeLa cells are highly proliferative, they should promote formation of new capillaries. Concurrently, angiogenesis was prominent in untreated eggs grafted with only HeLa cells, and the effect was considered 100% angiogenesis. This gradually decreased with increased concentrations of NP. The group of 100 µg NP/egg had significantly

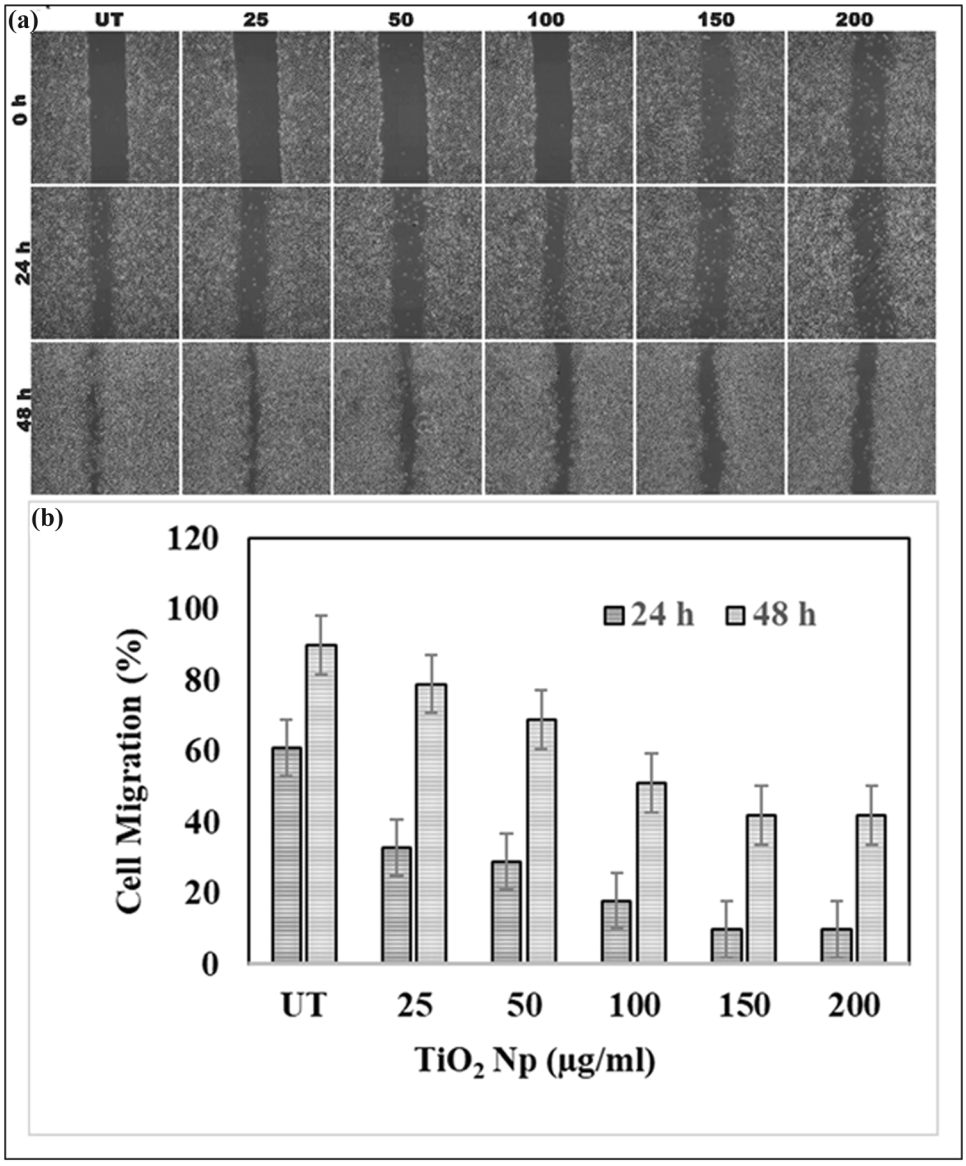

Figure 7: Effect of biogenic TiO_2 NP on HeLa Cell migration. HeLa cells were grown to 80% confluency and treated with varying concentrations of biogenic TiO_2 NP. *In vitro* wound healing assay was performed by making a straight-line scratch across the HeLa cell monolayer and the gap width of the wound was measured at 24 and 48 h time intervals. (a) Representative microscopic images (10× magnification) of wounds made and treated with varying TiO_2 NP concentrations, at 0, 24, and 48 h post treatment. (b) Quantification of the results.

reduced angiogenesis (20 ± 5%) [43]. NP controls did not show any toxicity against CAM of inoculated eggs with the survival rate of 90 ± 5%, which was like healthy untreated controls. These findings therefore indicate the anti-tumor, anti-proliferative, and anti-angiogenic properties of TiO_2 NP, comparable with NP synthesized from gold, selenium, silver, etc. [44]. As the study shows significant anti-cancer properties of the NP, they are safe and strong candidates for formulating anti-cancer molecules, possibly, also for coating or tagging with other anti-cancer drugs, such as DX, for synergistic effect [39].

3.11 Conjugation with TiO_2 NP enhanced DX and PTx toxicity against cancer cells

The shift in λ_{max} to longer wavelength (data not shown) was indicative of efficient and complete loading of DX and PTx on TiO_2 NP. To evaluate the cytotoxicity of various formulations against HeLa cells, the MTT assay was performed. HeLa cells were treated with TiO_2 NP, DX, DX NP, PTx, and PTx NP for 24 h. We observed anatase form exhibiting higher cytotoxicity than free DX or PTx. Further results indicate that the cytotoxicity of both

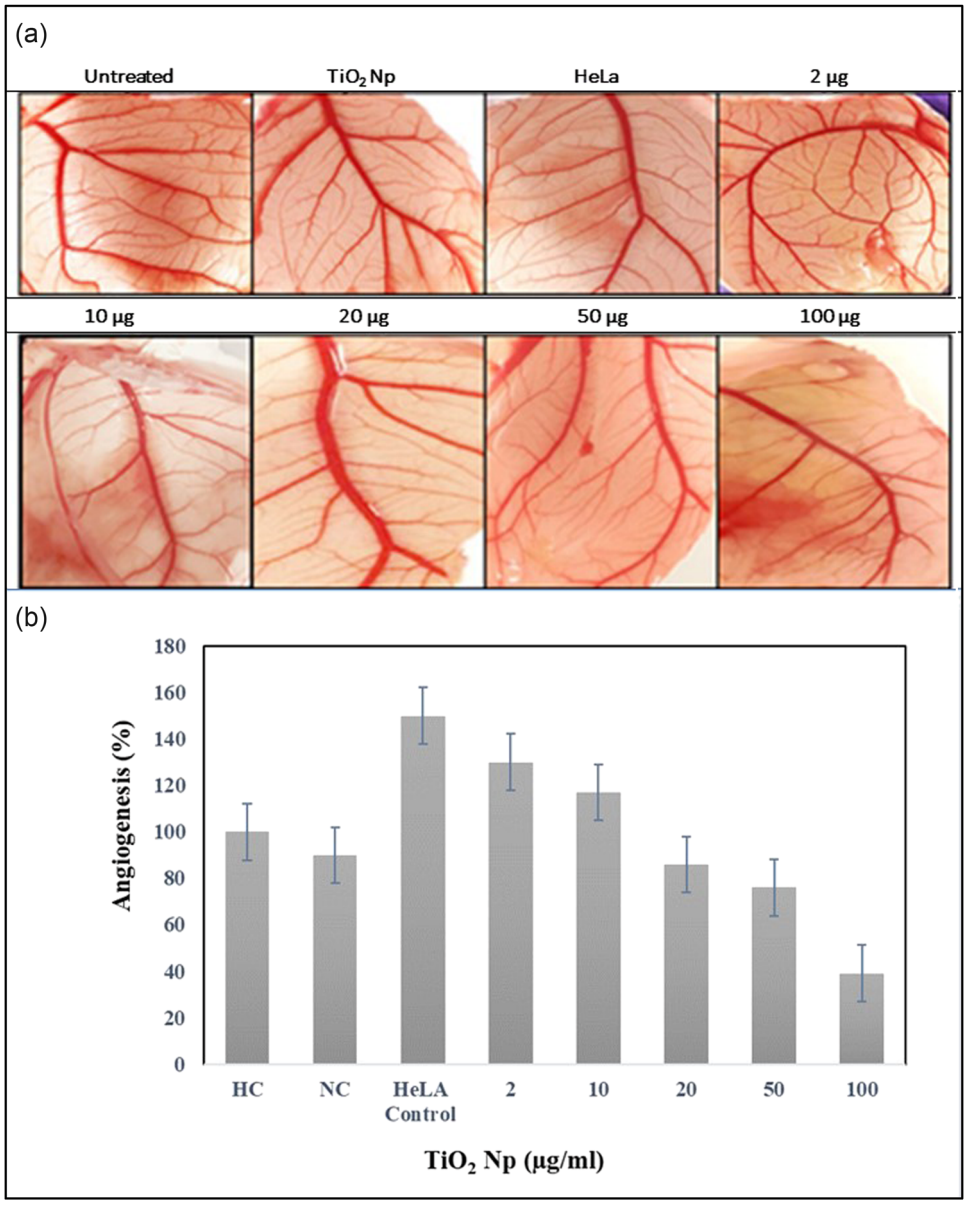

Figure 8: Assessment of anti-angiogenic property of biogenic TiO_2 NP using hen egg chorioallantoic membrane (CAM) assay. Eleven-day-old embryonated hen eggs were overlaid with HeLa cells in the presence or absence of biogenic TiO_2 NP and formation of new capillaries around the HeLa Cells grafted into the CAM layer was assessed under a dissection microscope at 5× magnification. Untreated: CAM layer inoculated with PBS; TiO_2 NP: (a) CAM layer inoculated with only TiO_2 NP; HeLa: CAM layer inoculated with only HeLa cells; 2–100 µg labeled panels: CAM layer inoculated with 2–100 µg TiO_2 NP along with HeLa cells. (b) Graphical representation of % angiogenesis.

nanoconjugates, i.e., DX NP and PTx NP, was higher than free drug as shown in Figure 9a and b. The cytotoxicity of 0.125 µM (125 nM) NP exhibited around 77 ± 5%. Free DX at lower concentrations showed less cytotoxicity compared to DX NP which showed cytotoxicity of 55 ± 5% at 0.009 µM itself. Free PTx even at higher concentration of 0.12 µM showed cytotoxicity of 24.7 ± 5%, whereas PTx NP conjugates showed relatively improved toxicity against HeLa cells with 70 ± 5% cytotoxicity at 0.12 µM. Previous studies with anatase form of TiO_2 NP conjugated to bioactive components like folic acid have been utilized for their enhanced activity to target cancer cells. In such studies, anatase form was utilized as it showed higher reactivity compared with bulk rutile form, which is also due to higher phototoxicity of the anatase form [45]. Current study confirms these observations as drug conjugated TiO_2 NP showed higher toxicity than unconjugated NP. The phototoxicity of the anatase form is due to the induction of ROS that may be contributing

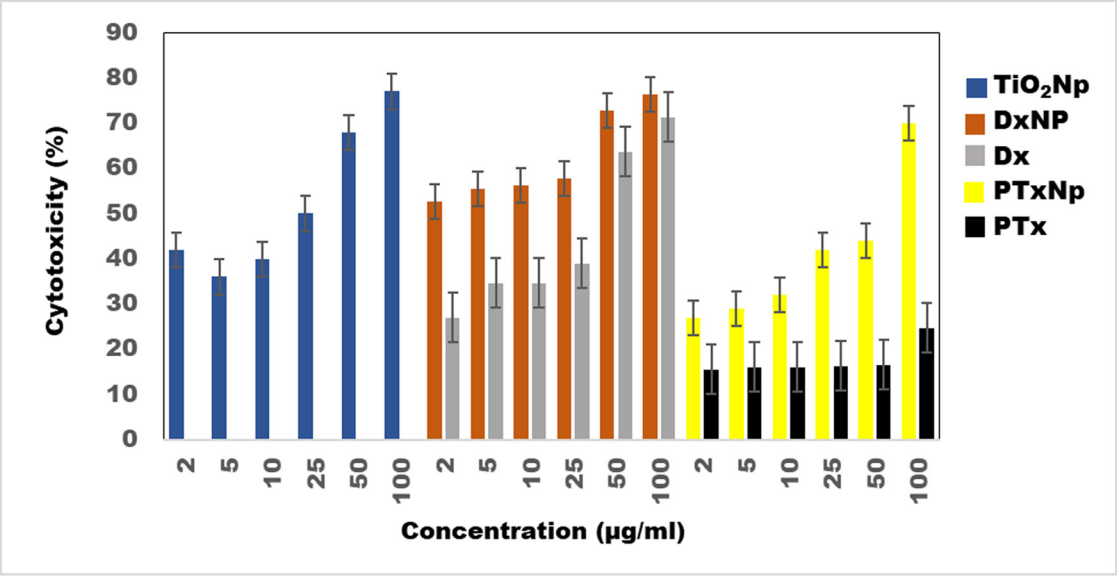

Figure 9: Graph depicting synergistic effect of conjugating biogenic TiO_2 with generic anti-cancer drugs DX and PTx on cell viability of cervical cancer cells (HeLa) as assessed by MTT assay. TiO_2 NP, Dx NP (DX-conjugated NP), DX (doxorubicin), PTx NP (PTx-conjugated NP), and PTx (paclitaxel).

to the enhanced cytotoxicity, indicating its potential application in chemotherapeutic drug formulations. Conjugation of TiO_2 NP to DX and PTx may also contribute to their synergistic effect in toxicity against cancer cells due to enhanced generation of destructive ROS [46].

4 Conclusion

The present study explores the synthesis and optimization of TiO_2 NP from *E. aestuarii*. TiO_2 is one of the most studied photocatalytic materials due to its abundance, stability, and relatively cheaper cost. Mainly, the optimization of stable bulk anatase form was observed by pH-based synthesis for enhanced stability and biological activity. It exists mainly in anatase, rutile, and brookite form in nature. Out of these, the anatase form has high photocatalytic reactivity and consequently, high biological activity. It is particularly stable and has high reactivity in nanoscale range (101) and (001) [37].

The bulk anatase form optimized in this study interestingly showed toxicity against cancer cells in terms of migration, clonogenicity, and inhibition of angiogenesis. Anatase form of TiO_2 NP showed significant inhibition of invasiveness of HeLa cells in terms of migration and proliferation in culture and by reducing their reproductive efficiency. CAM assay confirmed that the probable mechanism of anti-proliferative and anti-angiogenic activities of the anatase form of TiO_2 NP was via an increase in ROS generation leading to cell death. Low cytotoxicity of both rutile and anatase NP against the normal cell line HFF also suggests their potential application in formulating new anti-cancer drugs and designing targeted drug delivery system with minimum or no side effects on normal cells or organs. By optimization of conditions for obtaining bulk anatase form, we have improved the biological activity of the TiO_2 NP. We could also stabilize the rutile form which is inert and has least toxicity against cancer cells. These two forms can be useful for diverse applications. Specifically, bulk anatase form has good cytotoxicity against cancer cells, particularly cervical cancer cells (HeLa), suggesting potential application in designing NP-tagged anti-tumor drugs for targeting cancer cells with minimum toxicity against healthy blood cells. Furthermore, synergetic effect of NP tagged with DX and PTx, which are known cancer drugs, against cancer cells, when compared to free DX or PTx, was observed. This has important implications, as toxicity against healthy cells is a major challenge in designing anti-cancer drugs, which are generally shown to have severe side effects. In conclusion, further testing of generic anti-cancer drugs tagged with anatase TiO_2 NP opens promising avenues for targeting cervical cancer cells.

Acknowledgments: The authors are thankful to Professor Surya Satyanarayana Singh, Former Director, CFRD, Osmania University, Hyderabad, India, for providing technical support for the study.

Funding information: The authors state no funding involved.

Author contributions: MVSS, CLK, SB, and FS designed the study, MVSS, CLK, RK, KR, and APK acquired the data, MVSS, CLK, SNK, SB, and FS analyzed the data, MVSS, CLK, SB, and FS wrote the manuscript. MVSS and CLK gave equal contribution.

Conflict of interest: The authors state no conflict of interest.

Data availability statement: The datasets generated during and/or analyzed during the current study are available from the corresponding author on reasonable request.

References

[1] Griffitt R, Luo J, Gao J, Bonzongo J, Barber D. Effects of particle composition and species on toxicity of metallic nanomaterials in aquatic organisms. Environ Toxicol Chem. 2008;27(9):1972. doi: 10.1897/08-002.1.

[2] Zhang X, Yan S, Tyagi R, Surampalli R. Synthesis of nanoparticles by microorganisms and their application in enhancing microbiological reaction rates. Chemosphere. 2011;82(4):489–94. doi: 10.1016/j.chemosphere.2010.10.023.

[3] Waghmode M, Gunjal A, Mulla J, Patil N, Nawani N. Studies on the titanium dioxide nanoparticles: Biosynthesis, applications, and remediation. SN Appl Sci. 2019;1(4). doi: 10.1007/s42452-019-0337-3.

[4] Poulopoulos S, Yerkinova A, Ulykbanova G, Inglezakis V. Photocatalytic treatment of organic pollutants in a synthetic wastewater using UV light and combinations of TiO2, H2O2 and Fe(III). PLoS One. 2019;14(5):e0216745. doi: 10.1371/journal.pone.0216745.

[5] Albanese A, Tang P, Chan W. The effect of nanoparticle size, shape, and surface chemistry on biological systems. Ann Rev Biomed Eng. 2012;14(1):1–16. doi: 10.1146/annurev-bioeng-071811-150124.

[6] Kirthi A, Rahuman A, Rajakumar G, Marimuthu S, Santhoshkumar T, Jayaseelan C, et al. Biosynthesis of titanium dioxide nanoparticles using bacterium Bacillus subtilis. Mater Lett. 2011;65(17–18):2745–7. doi: 10.1016/j.matlet.2011.05.077.

[7] Rajakumar G, Rahuman A, Priyamvada B, Khanna V, Kumar D, Sujin P. Eclipta prostrata leaf aqueous extract mediated synthesis of titanium dioxide nanoparticles. Mater Lett. 2012;68:115–7. doi: 10.1016/j.matlet.2011.10.038.

[8] Prasad K, Jha A. Biosynthesis of CdS nanoparticles: An improved green and rapid procedure. J Colloid Interface Sci. 2010;342(1):68–72. doi: 10.1016/j.jcis.2009.10.003.

[9] Feng H. Green biosynthesis of CdS nanoparticles using yeast cells for fluorescence detection of nucleic acids and electrochemical detection of hydrogen peroxide. Int J Electrochem Sci. 2017;12(1):618–28. doi: 10.20964/2017.01.57.

[10] Singh J, Kumar S, Alok A, Upadhyay S, Rawat M, Tsang D, et al. The potential of green synthesized zinc oxide nanoparticles as nutrient source for plant growth. J Clean Prod. 2019;214:1061–70. doi: 10.1016/j.jclepro.2019.01.018.

[11] Uboldi C, Urbán P, Gilliland D, Bajak E, Valsami-Jones E, Ponti J, et al. Role of the crystalline form of titanium dioxide nanoparticles: Rutile, and not anatase, induces toxic effects in Balb/3T3 mouse fibroblasts. Toxicol Vitr. 2016;31:137–45. doi: 10.1016/j.tiv.2015.11.005.

[12] Sandhya M, Rajkumar K, Burgula S. Efficient eco-friendly approach towards bimetallic nanoparticles synthesis and characterization using Exiguobacterium aestuarii by statistical optimization. Green Chem Lett Rev. 2019;12(4):420–34. doi: 10.1080/17518253.2019.1687762.

[13] Lagopati N, Kitsiou P, Kontos A, Venieratos P, Kotsopoulou E, Kontos A, et al. Photo-induced treatment of breast epithelial cancer cells using nanostructured titanium dioxide solution. J Photochem Photobiol A Chem. 2010;214(2–3):215–23. doi: 10.1016/j.jphotochem.2010.06.031.

[14] Shi H, Magaye R, Castranova V, Zhao J. Titanium dioxide nanoparticles: a review of current toxicological data. Part Fibre Toxicol. 2013;10(1). doi: 10.1186/1743-8977-10-15.

[15] Deng W, Liu Y, Zhang Y, Lu F, Chen Q, Ji X. Enhanced electrochemical capacitance of nanoporous NiO based on an eggshell membrane. RSC Adv. 2012;2(5):1743. doi: 10.1039/C2RA00885H.

[16] Kumar A, Ma H, Zhang X, Huang K, Jin S, Liu J, et al. Gold nanoparticles functionalized with therapeutic and targeted peptides for cancer treatment. Biomater. 2012;33(4):1180–9. doi: 10.1016/j.biomaterials.2011.10.058.

[17] Abdelwahed W, Degobert G, Stainmesse S, Fessi H. Freeze-drying of nanoparticles: Formulation, process and storage considerations. Adv Drug Deliv Rev. 2006;58(15):1688–713. doi: 10.1016/j.addr.2006.09.017.

[18] Rohan S, Daniel E, Enzo P, Ian H. Optimisation and stability assessment of solid lipid nanoparticles using particle size and zeta potential. J Phys Sci. 2014;25(1):59–75.

[19] Ramkumar K, Manjula C, GnanaKumar G, Kanjwal M, Sekar T, Paulmurugan R, et al. Oxidative stress-mediated cytotoxicity and apoptosis induction by TiO_2 nanofibers in HeLa cells. Eur J Pharm Biopharm. 2012;81(2):324–33. doi: 10.1016/j.ejpb.2012.02.013.

[20] Rafehi H, Orlowski C, Georgiadis GT, Ververis K, El-Osta A, Karagiannis TC. Clonogenic assay: Adherent cells. J Vis Exp. 2011 Mar;49:2573. doi: 10.3791/2573.

[21] Liang CC, Park AY, Guan JL. In vitro scratch assay: A convenient and inexpensive method for analysis of cell migration in vitro. Nat Protoc. 2007;2(2):329–33. doi: 10.1038/nprot.2007.30.

[22] Zheng W, Yang L, Liu Y, Qin X, Zhou Y, Zhou Y, et al. Mo polyoxometalate nanoparticles inhibit tumor growth and vascular endothelial growth factor induced angiogenesis. Sci Tech Adv Mater. 2014;15:035010. doi: 10.1088/1468-6996/15/3/035010.

[23] Dhamecha D, Jalalpure S, Jadhav K. Doxorubicin functionalized gold nanoparticles: Characterization and activity against human cancer cell lines. Process Biochem. 2015;50(12):2298–306. doi: 10.1016/j.procbio.2015.10.007.

[24] Lin X, Li J, Ma S, Liu G, Yang K, Tong M, et al. Toxicity of TiO_2 nanoparticles to Escherichia coli: Effects of particle size, crystal phase and water chemistry. PLoS One. 2014;9(10):e110247. doi: 10.1371/journal.pone.0110247.

[25] Jiang J, Oberdörster G, Biswas P. Characterization of size, surface charge, and agglomeration state of nanoparticle dispersions for toxicological studies. J Nanopart Res. 2008;11:77–89. doi: 10.1007/s11051-008-9446-4.

[26] Das S, Ng WK, Tan RB. Are nanostructured lipid carriers (NLCs) better than solid lipid nanoparticles (SLNs): development, characterizations and comparative evaluations of clotrimazole-loaded SLNs and NLCs? Eur J Pharm Sci. 2012 Aug;47(1):139–51. doi: 10.1016/j.ejps.2012.05.010.

[27] Honary S, Zahir F. Effect of zeta potential on the properties of nano-drug delivery systems – A review (Part 2). Trop J Pharm Res. 2013;12(2). doi: 10.4314/tjpr.v12i2.19.
[28] Ghosh M, Chakraborty A, Mukherjee A. Cytotoxic, genotoxic and the hemolytic effect of titanium dioxide (TiO_2) nanoparticles on human erythrocyte and lymphocyte cellsin vitro. J Appl Toxicol. 2013;33(10):1097–110. doi: 10.1002/jat.2863.
[29] Stiufiuc R, Iacovita C, Nicoara R, Stiufiuc G, Florea A, Achim M, et al. One-step synthesis of PEGylated gold nanoparticles with tunable surface charge. J Nanomater. 2013;2013:1–7. doi: 10.1155/2013/146031.
[30] Karimian H, Babaluo A. Halos mechanism in stabilizing of colloidal suspensions: Nanoparticle weight fraction and pH effects. J Eur Ceram Soc. 2007;27(1):19–25. doi: 10.1016/j.jeurceramsoc.2006.05.109.
[31] Sastry M, Ahmad A, Khan MI, Kumar R. Microbial nanoparticle production. In: Niemeyer CM, Mirkin CA, editors. Nanobiotech. Weinheim: Wiley-VCH; 2004.
[32] Nam S, Parikh D, Condon B, Zhao Q, Yoshioka-Tarver M. Importance of poly(ethylene glycol) conformation for the synthesis of silver nanoparticles in aqueous solution. J Nanopart Res. 2011;13(9):3755–64. doi: 10.1007/s11051-011-0297-z.
[33] Chahardoli A, Haghighi ZMS, Shokoohinia Y, Fattahi A. Plant based biosynthesis of TiO2 NPs and evaluation of their cytotoxicity, anti-hemolytic, and protein antidenaturation effects. S Afr J Bot. 2023;163:37–44. doi: 10.1016/j.sajb.2023.10.028.
[34] Chahardoli A, Qalekhani F, Shokoohinia Y, Fattahi A. Caffeic acid based titanium dioxide nanoparticles: Blood compatibility, anti-inflammatory, and cytotoxicity. J Mol Liq. 2022;361:119674. doi: 10.1016/j.molliq.2022.119674.
[35] Chahardoli A, Hosseinzadeh L, Shokoohinia Y, Fattahi A. Production of rutile titanium dioxide nanoparticles by trans-ferulic acid and their biomedical applications. Mater Today Commun. 2022;33:104305. doi: 10.1016/j.mtcomm.2022.104305.
[36] Chahardoli A, Jalilian F, Shokoohinia Y, Fattahi A. The role of quercetin in the formation of titanium dioxide nanoparticles for nanomedical applications. Toxicol Vitro. 2023;87:105538. doi: 10.1016/j.tiv.2022.105538.
[37] Lambert AW, Pattabiraman DR, Weinberg RA. Emerging biological principles of metastasis. Cell. 2017 Feb;168(4):670–91. doi: 10.1016/j.cell.2016.11.037.
[38] Mohammad GRKS, Tabrizi MH, Ardalan T, Yadamani S, Safavi E. Green synthesis of zinc oxide nanoparticles and evaluation of anti-angiogenesis, anti-inflammatory and cytotoxicity properties. J Biosci. 2019;44. doi: 10.1007/s12038-019-9845-y.
[39] Vu BT, Shahin SA, Croissant J, Fatieiev Y, Matsumoto K, Le-Hoang Doan T, et al. Chick chorioallantoic membrane assay as an in vivo model to study the effect of nanoparticle-based anticancer drugs in ovarian cancer. Sci Rep. 2018 Jun;8(1):8524. doi: 10.1038/s41598-018-25573-8.
[40] Meyer SE, Hasenstein JR, Baktula A, Velu CS, Xu Y, Wan H, et al. Kruppel-like factor 5 is not required for K-RasG12D lung tumorigenesis, but represses ABCG2 expression and is associated with better disease-specific survival. Am J Pathol. 2010 Sep;177(3):1503–13. doi: 10.2353/ajpath.2010.090651.
[41] Zhang H, Wang C, Chen B, Wang X. Daunorubicin-TiO2 nanocomposites as a "smart" pH-responsive drug delivery system. Int J Nanomed. 2012;7:235–42. doi: 10.2147/IJN.S27722.
[42] Wang F, Chen L, Zhang R, Chen Z, Zhu L. RGD peptide conjugated liposomal drug delivery system for enhance therapeutic efficacy in treating bone metastasis from prostate cancer. J Control Rel. 2014 Dec;196:222–33. doi: 10.1016/j.jconrel.2014.10.012.
[43] Aravind M, Amalanathan M, Mary MSM. Synthesis of TiO_2 nanoparticles by chemical and green synthesis methods and their multifaceted properties. SN Appl Sci. 2021;3:409. doi: 10.1007/s42452-021-04281-5.
[44] Ziental D, Czarczynska-Goslinska B, Mlynarczyk DT, Glowacka-Sobotta A, Stanisz B, Goslinski T, et al. Titanium dioxide nanoparticles: prospects and applications in medicine. Nanomaterials (Basel). 2020 Feb;10(2):387. doi: 10.3390/nano10020387.
[45] Chen S, Guo Y, Zhong H, Chen S, Li J, Ge Z, et al. Synergistic antibacterial mechanism and coating application of copper/titanium dioxide nanoparticles. Chem Eng J. 2014;256:238–46. doi: 10.1016/j.cej.2014.07.006.
[46] Araujo-Lopez E, Varilla LA, Seriani N, Montoya JA. TiO2 anatase's bulk and (001) surface, structural and electronic properties: A DFT study on the importance of Hubbard and van der Waals contributions. Surf Sci. 2016;653:187–96. doi: 10.1016/j.susc.2016.07.003.